

# Development of a new state-of-the-art beamline optimized for monochromatic single-crystal and powder X-ray diffraction under extreme conditions at the ESRF

M. Mezouar,\* W. A. Crichton, S. Bauchau, F. Thurel, H. Witsch, F. Torrecillas, G. Blattmann, P. Marion, Y. Dabin, J. Chavanne, O. Hignette, C. Morawe and C. Borel

European Synchrotron Radiation Facility, BP 220, 38043 Grenoble, France.  
E-mail: mezouar@esrf.fr

A new state-of-the-art synchrotron beamline fully optimized for monochromatic X-ray diffraction at high pressure and high (or low) temperature is presented. In comparison with the old high-pressure beamline ID30, this new beamline exhibits outstanding performance in terms of photon flux and focusing capabilities. The main components of this new instrument will be described in detail and compared with the performance of beamline ID30. In particular, the choices in terms of X-ray source, X-ray optics, sample environment and detectors are discussed. The first results of the beamline commissioning are presented.

© 2005 International Union of Crystallography  
Printed in Great Britain – all rights reserved

**Keywords:** synchrotron beamline; X-ray diffraction; high pressure.

## 1. Introduction

The investigation of matter under extreme conditions is one of the natural issues addressed at a synchrotron radiation source (Shimomura *et al.*, 1992; Nelmes & McMahon, 1994). Indeed, the highly collimated and intense X-ray beam available at the ESRF is the ideal tool for probing microscopic samples at maximum pressures and temperatures and for reducing the effects of gradients in these variables. At the ESRF, such microbeam techniques were first used at beamline ID9 for a variety of high-pressure experiments, including very challenging experiments such as single-crystal X-ray diffraction (XRD) of hydrogen above 1 Mbar (Loubeyre *et al.*, 1996) and high-resolution powder XRD of molecular oxygen (Akahama *et al.*, 1995). Owing to this success and to the increasing demand of beam time for high-pressure experiments, it was decided to build ID30, a second beamline fully dedicated to this topic. This highly specialized beamline was in operation from June 1996 and stopped its activity in August 2004. This instrument was dedicated 25% to high-pressure large-volume experiments in the Paris–Edinburgh cell (Besson *et al.*, 1992) and 75% to high-pressure diamond cell experimentation (Fourme *et al.*, 2001). The large-volume programme at ID30 was focused on measurements of phase equilibria (Crichton, Vaughan & Mezouar, 2001), thermo-elastic properties of solids (Stolen *et al.*, 2000) and more recently on the structures of melts and glasses (Crichton, Mezouar *et al.*, 2001) and *in situ* chemistry at high pressures and temperatures (Solozhenko *et*

*al.*, 2002). The diamond-cell facility was optimized for accurate structure determinations at ultrahigh pressures (Akahama *et al.*, 2002) and allowed simultaneous laser or resistive heating under pressure and temperature conditions that reproduce those of planetary interiors (Schultz *et al.*, 2005; Andrault *et al.*, 1997). Two-thirds of the user beam was dedicated to materials science experiments, with the remainder devoted to geophysical applications. This beamline was fully optimized for polychromatic powder and single-crystal X-ray diffraction. With the increasing demand for high-resolution monochromatic X-ray diffraction experiments, ID30 has been progressively converted into a monochromatic beamline but with some important limitations owing to the initial choices in terms of X-ray source, X-ray optics, sample environment and detectors that were optimized for polychromatic XRD. For this reason, a significant effort has been made to undertake the building of a new instrument, ID27, fully optimized for monochromatic high-resolution XRD under extreme pressure and temperature. The main components of this new beamline are presented in the following.

## 2. Experimental set-up

### 2.1. General beamline description

A general view of beamline ID27 is presented in Fig. 1. It is composed of an optical hutch, two specialized experimental hutches, two control cabins and two high-pressure labora-

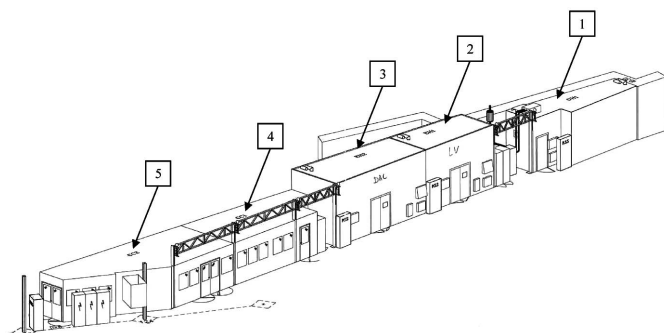


**Figure 1**  
General beamline overview. 1: optics hatch; 2: experimental hatch 1; 3: experimental hatch 2; 4: DAC laboratory; 5: P-E press laboratory.

tories. The first experimental hatch, EH1, is 6 m long and 2.5 m wide (on average) and is fully dedicated to large-volume-cell experiments using a Paris–Edinburgh (P–E) or equivalent press. The second hatch, EH2, is 8 m long and 3 m wide and is fully optimized for diamond-anvil cell (DAC) experiments at high temperature using laser or resistive heating and at low temperature using helium flow cryostats. Two sample preparation laboratories adapted to diamond-cell and large-volume-cell loading are located at the beamline for convenience. The centres of the experimental hatches EH1 and EH2 are respectively located at 41 and 48 m from the X-ray source. This X-ray source is composed of two small-gap in-vacuum undulators of period 23 mm that can be used simultaneously at a minimum magnetic gap of 6 mm. The monochromatic beam is selected using a nitrogen-cooled Si(111) monochromator and focused on the sample using multilayer mirrors in the Kirkpatrick–Baez (KB) geometry. EH1 and EH2 are respectively equipped with an XYZ translation to accommodate the P–E press and a versatile high-precision two-circle diffractometer suitable for powder and single-crystal diffraction in DACs. The diffraction signal is collected on a Bruker CCD detector or a MAR345 image plate that are easily interchanged using high-precision motorized translations.

## 2.2. The X-ray source

A very intense and highly focused X-ray beam is crucial for *in situ* diffraction experiments at high pressure because of the very small sample dimensions. For pressures above 100 GPa, the typical sample dimensions are of the order of 20  $\mu\text{m}$  or smaller. Moreover, high-pressure diffraction experiments require high photon flux at high X-ray energies because of the limited X-ray aperture of high-pressure cells and the highly absorbing pressure windows. Therefore, the choice of an optimized X-ray source is of primary importance (Chavanne *et al.*, 1998). Beamline ID30 was equipped with three insertion devices on a high- $\beta$  section (large source with a very small divergence in the horizontal direction), two wide-gap undulators with 35 and 40 mm periods, and one wiggler of period 70 mm. The minimum gap of these IDs was 16 mm, a limit imposed by the vacuum chamber dimension. These IDs were

**Table 1**  
Source characteristics of beamlines ID30 and ID27.

	Direction	Size (FWHM) ( $\mu\text{m}$ )	Divergence (FWHM) ( $\mu\text{rad}$ )
ID30	X (horizontal)	910	25
	Z (vertical)	30	5
ID27	X (horizontal)	134	208
	Z (vertical)	24	12

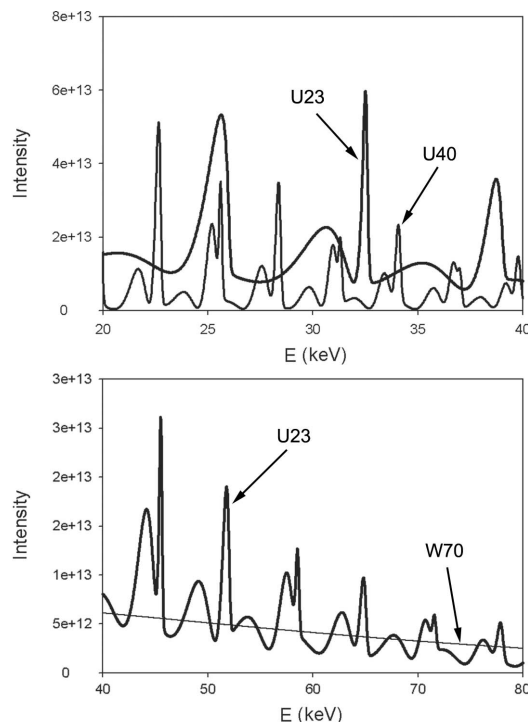


**Figure 2**  
Comparison of the insertion devices of ID27 and ID30 in the 20–40 keV and 40–80 keV X-ray energy domains.

chosen for their complementarities: the undulators provide high photon flux in the low-energy domain below 30 keV for monochromatic experiments and the wiggler provides a flat white-beam energy spectrum to energies higher than 100 keV suitable for polychromatic and high-energy monochromatic experiments. Beamline ID27 is upgraded with two in-vacuum small-gap undulators on a low- $\beta$  section (small source but higher divergence in the horizontal direction). The energy dependence of the photon intensity for the U23 in-vacuum undulators installed at beamline ID27 and of undulator U40 and wiggler W70 of beamline ID30 are compared in Fig. 2. The calculation was conducted for an incident beam size of 1 mm in the horizontal direction and 0.5 mm in the vertical direction at 30 m from the source. The two U23 undulators available at ID27 can reach minimum magnetic gaps of 6 mm and generate extremely bright beams in the X-ray energy region of interest. The intensity gain over beamline ID30 varies between 3 and 4 in the X-ray energy domain between 30 keV and 50 keV, which is the optimum energy region for high-pressure diffraction experiments. The source size and divergence at ID30 and ID27 are also compared in Table 1. The source at ID27 is approximately seven times smaller than the source at

ID30 in the horizontal direction, which allows a much better micro-focusing in this direction.

### 2.3. X-ray optics for high-pressure diffraction

The X-ray optics installed at beamline ID27 are based on the same principle as ID30 because of their simplicity and flexibility. The optical elements are composed of a channel-cut Si(111) monochromator located in the optics hutch at 30 m from the source and a pair of multilayer mirrors in the KB geometry installed in each experimental hutch to focus the monochromatic beam on the pressurized sample. Compared with ID30, significant improvements have been made: the water-cooled channel-cut Si(111) monochromator available at ID30 is replaced by a more efficient nitrogen-cooled monochromator (Zhang *et al.*, 2003) because of the high heat load generated by the two in-vacuum undulators. The dimensions of this monochromator are optimized to select a broad energy domain from 6 keV ( $\lambda = 2 \text{ \AA}$ ) to 90 keV ( $\lambda = 0.14 \text{ \AA}$ ) which largely covers the energy band needed for high-pressure diffraction experiments. The measured undulator spectrum in the energy range from 15 keV to 70 keV is presented in Fig. 3. The shape and position of the measured undulator harmonics are in good agreement with the calculated spectrum.

As already mentioned, the quality of focusing optics at high X-ray energies is of primary importance in high-pressure experiments because of the very small sample volume. The 170 mm-long multilayer mirrors of ID30 were upgraded to a pair of 300 mm-long mirrors at ID27, developed by the ESRF optics group (Hignette *et al.*, 2003). These multilayer mirrors are made of iridium–alumina multilayers deposited on silicon wafers. These mirrors possess a very broad energy band pass from 6 keV to 80 keV with a maximum of 80% reflectivity at 30 keV. A photograph of these new mirrors is shown in Fig. 4. Large focal distances of 800 mm and 1200 mm are used for the horizontal and the vertical mirrors, respectively, in order to avoid serious loss of spatial resolution. The optical acceptance of these new mirrors is 70% greater than that of the 170 mm mirrors, giving a substantial gain in photon flux. Moreover,

their alignment is simple and fast (less than 1 h) and they are mechanically very stable. The focal spot measured during the first test is shown in Fig. 5: a 6  $\mu\text{m}$  beam spot diameter at full width half-maximum (FWHM) was easily obtained.

### 2.4. Diffractometer and sample environment

**2.4.1. Pressure cells.** Two types of high-pressure cell are available for users and in-house research experiments at beamline ID27: the diamond and P–E cell. Static ultrahigh (Mbar) pressures are achieved in DACs that can concentrate high stresses to a very small area. Beamline ID27 has, together with beamline ID9, about ten DACs. Most of them are of the cylinder-piston type (LeToullec *et al.*, 1988; Chervin *et al.*, 1995) with a gas-driven membrane for pressure generation. These cells generally have 0.1 to 0.4 mm culet tips and are therefore suitable for generating pressures above 100 GPa. These cells can be used with simultaneous resistive heating to temperatures up to 1000 K, laser heating to temperatures above 3000 K or helium cryocooling to temperatures lower than 10 K. The P–E press can simultaneously generate stable pressures up to 8 GPa and temperatures up to 2200 K on sample volumes of several  $\text{mm}^3$  using tungsten carbide anvils (Mezouar *et al.*, 1999), and pressures up to 17 GPa and temperatures up to 1500 K using newly developed sintered diamond anvils. The P–E press is complementary to the DAC because of its much larger sample volume which, for instance, allows *in situ* chemistry at high pressure and high temperature with control of the stoichiometry (Nieto Sanz *et al.*, 2004).

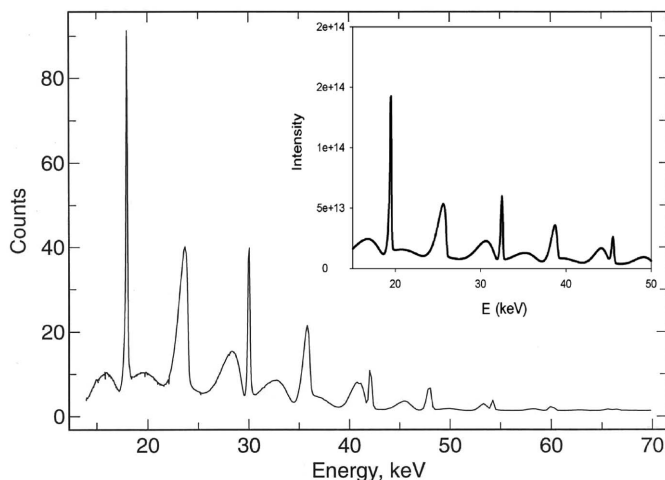


**Figure 3** Observed (main panel) and calculated (inset) spectra of the U23 undulator of ID27 in the energy domain from 15 to 70 keV.

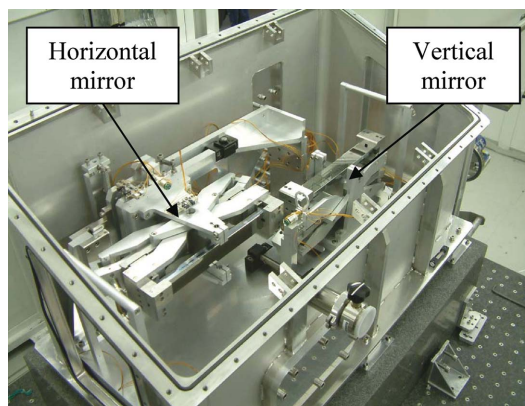


**Figure 4** Photograph of the pair of 300 mm-long KB mirrors.

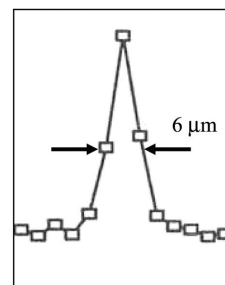


**Figure 5** Beam spot size along the horizontal direction measured by translating a tungsten wire at the focal point.

## SXD at Mbar pressures

**2.4.2. Diffractometer.** The large-volume-cell diffractometer is installed in a fully dedicated experimental hutch (EH1) and is composed of an *XYZ* cell stage that allows micro-positioning of the press, a Soller slits system (Mezouar *et al.*, 2002) to eliminate most of the background signal coming from the sample environment, and a large area detector (MAR345 or Bruker CCD), described below. The second experimental hutch is fully dedicated to DAC experiments and has a high-precision two-circle goniometer (rotations are about a vertical  $\omega$ -axis and a  $\chi$ -axis in the horizontal plane) installed on a stacking of three orthogonal translation tables *XYZ*. This goniometer can accommodate different types of DAC. Positioning (including that of independent-jaws micrometre-size slits) and centering the sample to an accuracy of better than 1  $\mu\text{m}$  is standard. The P-E cell and DAC diffractometers are both equipped with a photodiode mounted on a pneumatic actuator that sets it in or out of the X-ray beam. This photodiode, located between the pressure cell and the detector, is used for the initial centering of the pressure cells as well as for rapid checking of the alignment after each compression. Beamline ID27 is equipped with two X-ray detectors, namely a MAR345 image-plate scanner and a large-area Bruker CCD detector. The criteria for a detector suitable for high-pressure experiments are mostly dictated by the cell geometry (limited  $2\theta$  angle), composition (diamonds for the DACs, boron gaskets for the P-E press) and by working X-ray energies. These criteria impose a large input surface of more than 150 mm diameter, a high spatial resolution (point spread function of 150  $\mu\text{m}$  FWHM or less), low noise and high dynamic range (14 bits or more), a good sensitivity at high X-ray energies above 30 keV, and stable and easily tractable spatial distortions with fast reading (a few seconds or less) and erasing times. The MAR345 image-plate detector fulfils most of the above criteria but has a long readout time of 1 min or more depending on the choice of the pixel size. This becomes problematic when compared with exposure times of the order of 1 s or less owing to the high photon flux available at beamline ID27. The situation is improved with the large-area Bruker 6500 CCD detector because the readout time is reduced to 5 s in full binning. However, this detector has a poor dynamic range of only 13 bits which limits its use to high signal-to-noise ratio experiments such as single-crystal diffraction.

### 3. Beamline commissioning: first results

The beamline performances have been firstly tested on a lanthanum hexaboride powder ( $\text{LaB}_6$ ) sample (SRM 660a) from the National Institute of Standards and Technology (NIST, USA). The sample was loaded into a hole of diameter 150  $\mu\text{m}$  and thickness 40  $\mu\text{m}$  of an indented stainless steel gasket in order to reproduce the typical sample geometry in a DAC. The wavelength of the incident X-ray beam was 0.3738  $\text{\AA}$  which corresponds to the iodine *K*-edge, the standard wavelength used at beamline ID27 for DAC experiments. The exposure time was set using an electromechanical fast-shutter with a minimum opening/closing time of 10 ms. The

diffraction patterns were collected on a MAR345 image-plate scanner and circularly integrated using the software *Fit2D* (Hammersley *et al.*, 1996). A typical diffraction pattern of  $\text{LaB}_6$  and the corresponding one-dimensional spectrum is presented in Fig. 6; the sample-to-detector distance was approximately 360 mm. In this case, the focusing mirrors were not used; the X-ray beam was simply collimated down to 50  $\mu\text{m} \times 50 \mu\text{m}$  using a pair of tungsten carbide slits in order to prevent any contamination from the gasket material. The detector saturation was reached after only 5 s of exposure confirming the important gain in intensity. The relative *d*-spacing variation  $\Delta d/d$  obtained from the pseudo-Voigt fitting of the diffraction lines of the  $\text{LaB}_6$  pattern was  $\Delta d/d = 1.5 \times 10^{-4}$ . Another set of diffraction patterns were collected with the focusing mirrors in place in order to estimate the loss of spatial resolution that they induce. The focal spot diameter obtained with the KB mirrors was 7  $\mu\text{m}$  (FWHM) with an incident X-ray beam size of 0.5 mm  $\times$  0.8 mm. In this case, the exposure time was reduced to less than 1 s because of the large angular acceptance of the mirrors. The  $\Delta d/d$  value increased to  $3.1 \times 10^{-4}$  when the mirrors were employed. This degradation of the spatial resolution is an acceptable compromise for high-pressure diffraction experiments where focusing optics are mandatory.

In order to test further the instrument capabilities under real experimental conditions, we have performed a high-

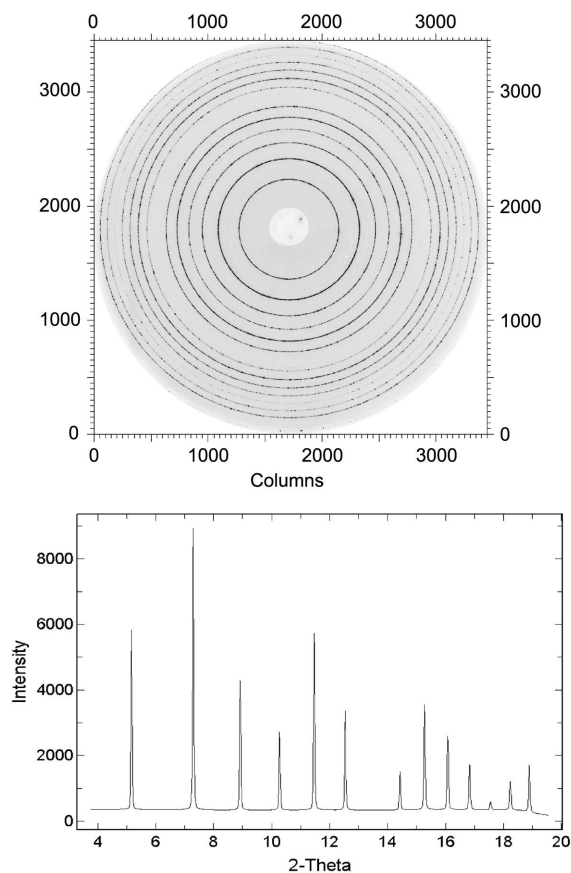


**Figure 6** Two-dimensional X-ray diffraction pattern of  $\text{LaB}_6$  (top) and the corresponding one-dimensional spectrum collected at ID27 (bottom).



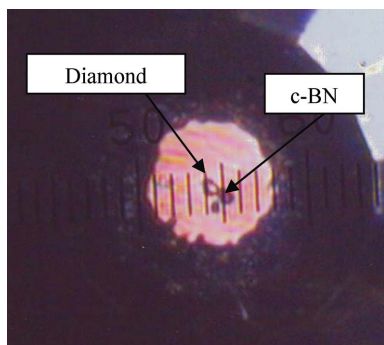


**Figure 7**  
Photograph of a gasket cavity that contains micro-crystals of c-BN and diamond and a ruby chip. The pressure medium is neon.

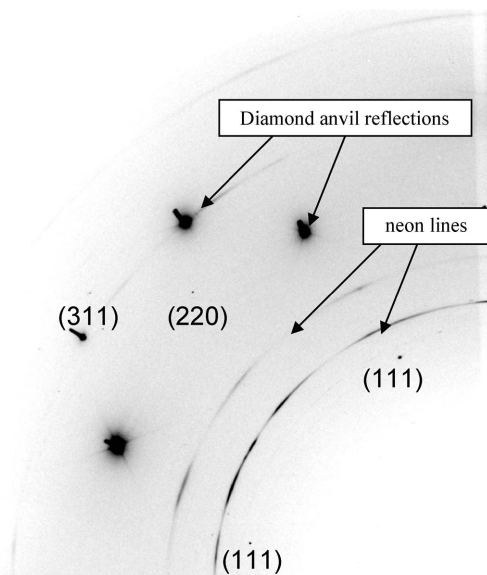


**Figure 8**  
A quarter of a two-dimensional diffraction pattern of c-BN and diamond collected at 72 GPa. The (111), (220) and (311) reflections of c-BN are indicated, together with the diamond-anvil reflections and neon rings.

pressure single-crystal diffraction on micro-samples of diamond and cubic boron nitride (c-BN). This experiment was an excellent bench test for the beamline performance since it accumulates numerous difficulties. Indeed, c-BN and diamond have low X-ray scattering power and the average size of the two micro-crystals was only of 5  $\mu\text{m}$  in the three directions. A photograph of the sample environment is presented in Fig. 7. The c-BN and diamond micro-crystals were loaded together with a ruby chip into a 40  $\mu\text{m}$  gasket hole. Neon was used as pressure medium in order to ensure good hydrostatic conditions and the pressure was measured using the ruby fluorescence method (Mao *et al.*, 1978). A typical diffraction image obtained at a pressure of 72 GPa is presented in Fig. 8. The single-crystal reflections of the c-BN sample and diamond anvils and the powder rings from neon are clearly visible. The saturation of the detector by the single-crystal reflection of c-BN and diamond was obtained after only 100 ms of exposure. No trace of gasket signal was observed even when the DAC was rotated by 40°. This confirms the tight beam focusing and the absence of an extended tail. These very first results are

very promising and open the door toward the collection of high-quality data in the multi-megabar regime.

#### 4. Conclusion

A new beamline for collecting high-quality diffraction data suitable for structural refinement under extreme pressures and temperatures has been built and successfully commissioned at the ESRF. All of the beamline components have been optimized for this specific application. The first results obtained on LaB<sub>6</sub>, c-BN and diamond demonstrate the great potential of this new instrument.

We are very grateful to the constant support from the ESRF directors and to the invaluable help from the ESRF support groups involved in the beamline construction. More particularly, we would like to thank P. Berkvens and P. Colomp from the safety group, N. Levet, D. Schirr-Bonnans, C. Lefebvre and G. Gatta from the survey group, W. Schmid and J.-L. Berclaz from the mechanical pool, J.-C. Laidet and O. Chamond from the technical services, and F. Bodart and J. L. Bersier from the vacuum group, who played a crucial role at different stages of the project. F. Datchi, A. Dewaele and Y. Le Godec are warmly thanked for providing the data on c-BN and diamond.

#### References

- Akahama, Y., Kawamura, H., Haeusermann, D., Hanfland, M. & Shimomura, O. (1995). *Phys. Rev. Lett.* **74**, 4690–4693.
- Akahama, Y., Kawamura, H. & Le Bihan, T. (2002). *J. Phys. Condens. Matter*, **14**, 10583–10588.
- Andraut, D., Fiquet, G., Kunz, M., Visocekas, F. & Haeusermann, D. (1997). *Science*, **278**, 831–834.
- Besson, J. M., Nemes, R. J., Hamel, G., Loveday, J. S., Weill, G. & Hull, S. (1992). *Physica B*, **180/181**, 907–910.
- Chavanne, J., Elleaume, P. & Van Vaerenbergh, P. (1998). *J. Synchrotron Rad.* **5**, 196–201.
- Chervin, J. C., Canny, B., Besson, J. M. & Pruzan, P. (1995). *Rev. Sci. Instrum.* **66**, 2595–2598.
- Crichton, W. A., Mezouar, M., Grande, T., Stolen, S. & Grzechnik, A. (2001). *Nature (London)*, **414**, 622–625.
- Crichton, W. A., Vaughan, G. B. M. & Mezouar, M. (2001). *Z. Kristallogr.* **216**, 417–419.
- Fourme, R., Kahn, R., Mezouar, M., Girard, E., Hoerentrup, C. & Ascone, I. (2001). *J. Synchrotron Rad.* **8**, 1149–1156.
- Hammersley, A. P., Svensson, S. O., Hanfland, M., Fitch, A. N. & Hausermann, D. (1996). *High Press. Res.* **14**, 235–248.
- Hignette, O., Cloetens, P., Lee, W. K., Ludwig, W. & Rostaing, G. (2003). *J. Phys. IV*, **104**, 231–234.
- Le Toullec, R., Pinceaux, J. P. & Loubeyre, P. (1988). *High Press. Res.* **1**, 77–81.
- Loubeyre, P., LeToullec, R., Hausermann, D., Hanfland, M., Hemley, R. J., Mao, H. K. & Finger, L. W. (1996). *Nature (London)*, **383**, 702–704.
- Mao, H. K., Bell, P. M., Shaner, J. W. & Steinberg, D. J. (1978). *J. Appl. Phys.* **49**, 3276–3283.
- Mezouar, M., Faure, P., Crichton, W., Rambert, N., Bauchau, S. & Blattmann, G. (2002). *Rev. Sci. Instrum.* **73**, 3770–3774.
- Mezouar, M., Le Bihan, T., Libotte, H., Le Godec, Y. & Haeusermann, D. (1999). *J. Synchrotron Rad.* **6**, 1115–1119.
- Nemes, R. J. & McMahon, M. I. (1994). *J. Synchrotron Rad.* **1**, 69–73.
- Nieto Sanz, D., Loubeyre, P., Crichton, W. A. & Mezouar, M. (2004). *Phys. Rev. B*, **70**, 214108–214114.

## SXD at Mbar pressures

---

- Schultz, E., Mezouar, M., Crichton, W. A., Bauchau, S., Blattmann, G., Andrault, D., Fiquet, G., Boehler, R., Rambert, N., Sitaud, B. & Loubeyre, P. (2005). *High Press. Res.* **25**, 71–83.
- Shimomura, O., Takemura, K., Fujihisa, H., Fujii, Y., Ohishi, Y., Kikegawa, T., Amemiya, Y. & Matsushita, T. (1992). *Rev. Sci. Instrum.* **63**, 967–973.
- Solozhenko, V. L., Turkevich, V. Z., Kurakevych, O. O., Crichton, W. A. & Mezouar, M. (2002). *J. Phys. Chem. B*, **106**, 6634–6637.
- Stolen, S., Grzechnik, A., Grande, T. & Mezouar, M. (2000). *Solid State Commun.* **115**, 249–252.
- Zhang, L., Lee, W. K., Wulff, M. & Eybert, L. (2003). *J. Synchrotron Rad.* **10**, 313–319.